

# Nuclear Magnetic Resonance of Hydrogen Bonded Clusters Between F<sup>-</sup> and (HF)<sub>n</sub>: Experiment and Theory

Ilja G. Shenderovich<sup>1,2</sup>, Sergei N. Smirnov<sup>1</sup>, Gleb S. Denisov<sup>1</sup>, Vladimir A. Gindin<sup>1</sup>, Nikolai S. Golubev<sup>1\*</sup>, Anita Dunger<sup>2</sup>, Rebecca Reibke<sup>2</sup>, Sheela Kirpekar<sup>3</sup>, Olga L. Malkina<sup>4</sup>, and Hans-Heinrich Limbach<sup>2\*</sup>

<sup>1</sup> Institute of Physics, St. Petersburg State University, 198904 St. Petersburg, Russian Federation

<sup>2</sup> Institut für Organische Chemie, Freie Universität Berlin, Takustraße 3, D-14195 Berlin, Germany

<sup>3</sup> University of Odense, Odense, Denmark

<sup>4</sup> Computing Center, Slovak Academy of Sciences, Bratislava, Slovakia

*Key Words:* Coupling Constants / Hydrogen Bonding / Spectroscopy, Nuclear Magnetic Resonance

Liquid state <sup>1</sup>H and <sup>19</sup>F NMR experiments in the temperature range between 110 and 150 K have been performed on mixtures of tetrabutylammonium fluoride with HF dissolved in a 1:2 mixture of CDF<sub>3</sub> and CDF<sub>2</sub>Cl. Under these conditions hydrogen bonded complexes between F<sup>-</sup> and a varying number of HF molecules were observed in the slow proton and hydrogen bond exchange regime. At low HF concentrations the well known hydrogen bifluoride ion [FHF]<sup>-</sup> is observed, exhibiting a strong symmetric H-bond. At higher HF concentrations the species [F(HF)<sub>2</sub>]<sup>-</sup>, [F(HF)<sub>3</sub>]<sup>-</sup> are formed and a species to which we assign the structure [F(HF)<sub>4</sub>]<sup>-</sup>. The spectra indicate a central fluoride anion which forms multiple hydrogen bonds to HF. With increasing number of HF units the hydrogen bond protons shift towards the terminal fluorine's. The optimized gas-phase geometries of [F(HF)<sub>n</sub>]<sup>-</sup>, n=1 to 4, calculated using ab initio methods confirm the D<sub>∞h</sub>, C<sub>2v</sub>, D<sub>3h</sub> and T<sub>d</sub> symmetries of these ions. For the first time, both one-bond couplings between a hydrogen bond proton and the two heavy atoms of a hydrogen bridge, here <sup>1</sup>J<sub>HF</sub> and <sup>1</sup>J<sub>HF'}</sub>, where <sup>1</sup>J<sub>HF</sub> ≥ <sup>1</sup>J<sub>HF'}</sub>, as well as a two-bond coupling between the heavy atoms, here <sup>2</sup>J<sub>FF</sub>, have been observed. The analysis of the differential width of various multiplet components gives evidence for the signs of these constants, i.e. <sup>1</sup>J<sub>HF</sub> and <sup>2</sup>J<sub>FF</sub> > 0, and <sup>1</sup>J<sub>HF'}</sub> < 0. Ab initio calculations of NMR chemical shifts and the scalar coupling constants using the Density Functional formalism and the Multi-configuration Complete Active Space method show a reasonable agreement with the experimental parameters and confirm the covalent character of the hydrogen bonds studied.

## 1. Introduction

The interaction of the fluoride ion with HF gives rise to anionic clusters of the type [F(HF)<sub>n</sub>]<sup>-</sup> which are ideal objects for theoretical, structural and spectroscopic studies of hydrogen bonding. Thus, anions with n=1 up to 5 have been studied by X-ray and neutron diffraction experiments [1]. Secondly, because of the small number of atoms in these complexes high level ab initio calculations of the isolated ions are possible from which not only electronic properties, energies and geometries, but also spectroscopic parameters can be obtained [2]. The hydrogen difluoride ion, [FHF]<sup>-</sup>, is known to involve the strongest and shortest hydrogen bond. The free ion is characterized according to gas phase data [3a,b] and ab initio calculations [2] by a symmetric single-well proton potential function, D<sub>∞h</sub> [3a,b]. In crystalline salts the symmetry of [FHF]<sup>-</sup> may be retained [1a,b,f,g,h] or lifted [1c,d,f,h] by the crystal field. The latter phenomenon leads to a lengthening of the hydrogen bond. Existing solid state NMR and neutron diffraction studies indicated a correlation between the F...F bond length and the proton position [1f], where shortest H-bond corresponds to a position of the proton at the hydrogen bond center. Both crystallographic and ab initio data show that the hydrogen bond symmetry is also lifted in the complexes [F(HF)<sub>n</sub>]<sup>-</sup>. The anions with n=2, 3 and 4 ex-

hibit C<sub>2v</sub> [1g, 1h, 2d]-, D<sub>3h</sub> [1g,h, 2d]- und T<sub>d</sub> [2d]-symmetries, with a central fluoride involved in multiple hydrogen bonds with more or less elongated HF units. These symmetries can be perturbed by changing the counterion [1h, 1i, 1k]. A general trend is that as n is increased the shorter F...H distances become shorter and the longer F...H longer. This phenomenon also leads to characteristic changes of the corresponding vibrational frequencies [1e, 2d].

By contrast, little is known about complexation of the fluoride ion by (HF)<sub>n</sub> in aprotic media. When dissolving a crystalline hydrogen-bonded salt of a definite composition, an equilibrium mixture of several complexes usually forms, and overlapping of their optical spectra makes it difficult to attribute vibrational bands [3c]. In the case of NMR experiments performed under conventional conditions, fast proton and hydrogen bond exchange averages the NMR signals of the various complexes preventing the observation of chemical shifts and coupling constants of the complexes [4]. In the past only for the most stable hydrogen difluoride ion well-resolved NMR spectra were obtained [5], exhibiting a scalar one-bond spin-spin coupling constant of <sup>1</sup>J<sub>HF</sub>=126 Hz. As this case constituted up to date the only example of scalar spin-spin coupling across an intermolecular hydrogen bond, the dependence of these couplings on the hydrogen bond properties were unknown. Moreover, the possibility of scalar two-bond F...F coupling in [FHF]<sup>-</sup> has never been considered to our knowledge as the corresponding coupling constant

\*) Authors for correspondence.

$^2J_{\text{FF}}$  cannot be measured by NMR spectra because of the magnetic equivalence of the two fluorine nuclei. By contrast, this coupling should be observable in the case of less symmetric ions, like  $[\text{F}(\text{HF})_n]^-$ ,  $n=2$  to 4, if it were possible to reach to slow-exchange regime of the various hydrogen bonded clusters.

These considerations incited us to become engaged in the study of the system tetrabutylammonium fluoride/HF, by means of the low-temperature (100–150 K) NMR technique using liquefied freons as solvents [6], allowing us to obtain high resolution spectra of hydrogen-bonded species in slow proton and hydrogen bond exchange regime. The results of this study are described in this paper. As expected, separate signals have been found for all hydrogen-bonded complexes,  $[\text{F}(\text{HF})_n]^-$ ,  $n=1$  to 4. Thus, not only all hydrogen and fluorine chemical shifts but also the one-bond  $^1\text{H}$ - $^{19}\text{F}$  and two bond  $^{19}\text{F}$ - $^{19}\text{F}$  couplings could be determined. In order to assist the correlation of the parameters observed with the hydrogen bond structures we have performed various ab initio calculations of optimized geometries, chemical shifts and coupling constants. In the next section the experiments and the computational methods are described. Then the result are presented and discussed.

## 2. Experimental

### 2.1 Sample Preparations and NMR-Experiments

As a low-temperature NMR solvent, a mixture of two freons,  $\text{CDF}_3/\text{CDF}_2\text{Cl}$ , with the freezing point below 100 K was used, prepared as described in Ref. [6b]. The solvent gives rise to a quartet in the  $^1\text{H}$  NMR spectrum at 6.52 ppm ( $\text{CHF}_3$ ) and a triplet at 7.18 ppm ( $\text{CHF}_2\text{Cl}$ ), where the signal intensities can be used to determine the exact composition. Usually, the ratio was about 1:2, but changes occurred which did, however, not lead to noticeable changes. No other  $^1\text{H}$  NMR signals could be observed for the pure solvent. The  $^{19}\text{F}$  spectrum exhibits very strong triplets at  $-78.6$  ppm for  $\text{CDF}_3$  and at  $-72.4$  ppm for  $\text{CDF}_2\text{Cl}$  (reference  $\text{CFCl}_3$ ). Additional  $^{19}\text{F}$  peaks are observed sometimes in the region of interest which are difficult to assign, arising from small amounts of so-far non-identified impurities. Part of these impurities comes either from the synthesis or from a reaction of fluoride with the inner glass surface. These impurities, did, however, not affect the characteristics of the reproducible lines assigned to the various species described below.

Tetrabutylammonium fluoride trihydrate (TBA, Fluka) and hydrofluoric acid (48% in water) from Aldrich were used for the sample preparation. The latter procedure consisted of the addition of the calculated amount of hydrofluoric acid to a fluorine solution in acetone and removing water by the azeotropic distillation with dichloromethane. Then the oily product was placed into a thick-wall Wilmad NMR sample tube (Buena, USA) equipped with a teflon needle valve, withstanding the pressure up

to 50 bars. The tube was connected to a high vacuum line and the solvent was added by vacuum transfer.

A number of different samples were prepared. The samples of which spectra are reported in this paper are sample #1 (concentrations TBA-F 0.020 M and HF 0.040, respectively), sample #2 (TBA-F 0.020 M and HF 0.017 M), sample #3 (TBA-F 0.020 M and HF 0.018 M) and sample #4 (TBA-F 0.020 M and HF 0.032 M).

The NMR spectra were recorded on a Bruker AMX-500 instrument supplied with a special NMR probehead allowing the temperature adjustment down to 96 K. The NMR chemical shifts were measured using the solvent peaks as internal reference and then converted into the usual scales.

### 2.2 Computational Methods

The optimized equilibrium geometries of ionic clusters were calculated using the GAUSSIAN 94 program [7] at the MP2/6-31+G(d,p) level. Calculations of chemical shifts and indirect spin-spin coupling constants using Density Functional theory (DFT) were performed with deMon-NMR code [8] according the computational procedure described in detail in Ref. [8]. Perdew and Wang exchange [9] with Perdew correlation [10] functionals and IGLO-III basis set [11] were implied. In DFT calculations FINE grid with 64 radial points was used for numerical integration [8d]. The absolute calculated shieldings were also referenced to tetramethylsilane in the case of  $^1\text{H}$  and  $\text{CFCl}_3$  in the case of  $^{19}\text{F}$ .

The multiconfiguration linear response (MCLR) calculations [12], using a MCSCF wavefunction of the complete active space type (CAS) [13], were carried out only for the  $[\text{FHF}]^-$ -system. For these calculations we used the DALTON program package [14]. As for the DFT calculations the basis set employed was the IGLO-III basis. The active space was chosen on the basis of the MP2 natural occupation numbers [15]. The inactive space contains the orbitals:  $1_g-2_g$ ;  $1_u-2_u$ , which are essentially the 1s- and 2s-orbitals on the fluorine atoms. The active space contains 13 orbitals:  $3_g-5_g$ ;  $3_u-4_u$ ;  $1_u-2_u$ ,  $1_g-2_g$  in which 12 active electrons are distributed. This leads to a total of 368 656 determinants.

## 3. Results

In this section we describe the results of the NMR experiments and of the computations. All results are assembled in Table 1.

### 3.1 Results of the NMR Experiments

#### 3.1.1 $^1\text{H}$ NMR Spectra

The  $^1\text{H}$  NMR spectra were found to be very sensitive to the relative concentrations of tetrabutylammonium fluoride and HF and the sample preparation. Nevertheless, reproducible results could be obtained. In Fig. 1 are de-

Table 1  
Calculated optimized geometries at the MP2/6-31+G(p,d) level and experimental and calculated NMR parameters of  $[\text{F}(\text{HF})_n]^-$

	$[\text{FHF}]^-$		$[\text{F}(\text{HF})_2]^-$		$[\text{F}(\text{HF})_3]^-$		$[\text{F}(\text{HF})_4]^-$	
Symmetry	$D_{\infty h}$		$C_{2v}$		$D_{3h}$		$T_d$	
$r(\text{F}-\text{H}), \text{\AA}$	1.1495		1.012		0.979		0.961	
$r(\text{F} \dots \text{H}), \text{\AA}$	1.1495		1.349		1.451		1.540	
$\alpha(\text{H}-\text{F}-\text{H})$	linear		$130.2^\circ$		$120.0^\circ$		$109.5^\circ$	
	exp.	calc.	exp.	calc.	exp.	calc.	exp. <sup>b</sup>	calc.
$\delta_{\text{H}}$ [ppm]	16.6	16.0	14.0	12.9	11.8	10.5	10.3 <sup>b</sup>	8.6
$\delta_{\text{F}}$ [ppm]	-155.4	-154.8	-148.9	-122.7	-147.2	-100.1	-	-82.5
$\delta_{\text{F}}$ [ppm]	-155.4	-154.8	-176.9	-153.9	-185.0	-156.9	-191.4 <sup>b</sup>	-159.0
$^1J_{\text{HF}}/\text{Hz}$	$124 \pm 3$	6, 133 <sup>a</sup>	$24 \pm 3$	-71	$41 \pm 4$	-72	$< 10^b$	-63.4
$^2J_{\text{FF}}/\text{Hz}$	-	-133, 385 <sup>a</sup>	$146 \pm 4$	-73	$92 \pm 5$	-100	$< 15^b$	-144
$^1J_{\text{HF}}'/\text{Hz}$	$124 \pm 3$	6, 133 <sup>a</sup>	$354 \pm 3$	229	$430 \pm 4$	300	$480 \pm 5^b$	336

Chemical shifts and coupling constant calculations: DFT method, <sup>a</sup> CAS-method. Standard for <sup>1</sup>H NMR is TMS, and for <sup>19</sup>F NMR  $\text{CFCl}_3$ . F': central fluorine, F: terminal fluorine's. <sup>b</sup> tentative assignment, for explanation see text.

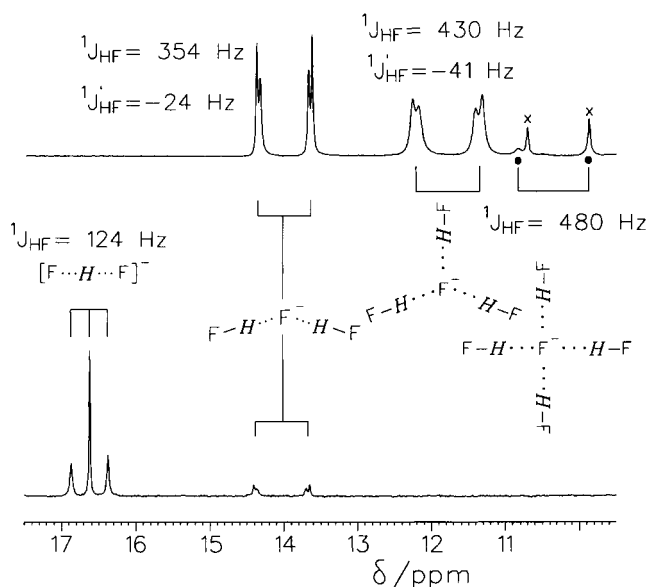


Fig. 1  
Low-field <sup>1</sup>H NMR signals (500 MHz) of solutions containing HF and tetrabutylammonium fluoride (sample #1, top) and (sample #2, bottom). Unidentified doublet marked by crosses

pictured the low-field <sup>1</sup>H NMR signals of two typical samples of tetrabutylammonium fluoride dissolved in  $\text{CDF}_3/\text{CDF}_2\text{Cl}$  (1:2) exhibiting different added amounts of HF and cooled down to 120 K. All signals arise from protons in  $\text{F} \dots \text{H} \dots \text{F}$  hydrogen bonds. At low HF concentration (sample 2, bottom), the well-known signal of  $[\text{FHF}]^-$  appearing at  $\delta = 16.6 \text{ ppm}$  is dominant, split into a triplet because of coupling with the two fluorine nuclei as described in Ref. [5]. Therefore, the corresponding one-bond coupling constants  $^1J_{\text{HF}}$  and  $^1J_{\text{HF}}' = 124 \text{ Hz}$  are identical. At higher HF concentrations (sample 1, top) additional multiplets observed at 14.0 and 11.8 which we assign to the species  $[\text{F}(\text{HF})_2]^-$  and  $[\text{F}(\text{HF})_3]^-$ , formed by successive addition of HF to  $[\text{FHF}]^-$ . In addition, a so far

unidentified doublet marked by crosses are observed at 10.2 ppm. Hidden under this signal is an additional broader doublet marked by full circles which we tentatively assign to  $[\text{F}(\text{HF})_4]^-$ .

The signal splitting patterns observed are typical for first-order spin systems although, in principle, the structures indicated in Fig. 1 represent high order spin systems as they contain chemically equivalent but magnetically non-equivalent protons and fluorine's. The first order patterns arise from the fact that the coupling constants  $^2J_{\text{HH}}$ ,  $^3J_{\text{HF}}$  and  $^4J_{\text{FF}}$  are smaller than the experimental line width, as checked by appropriate lineshape simulations [16]. In contrast to  $[\text{FHF}]^-$ , for  $[\text{F}(\text{HF})_2]^-$  and  $[\text{F}(\text{HF})_3]^-$  the two one-bond coupling constants  $^1J_{\text{HF}}$  and  $^1J_{\text{HF}}'$  are no longer identical (Table 1), indicating the presence of asymmetric hydrogen bonds characterized by a smaller F-H and a larger  $\text{F} \dots \text{H}$  distance. Moreover, only one signal is observed for each species which can be explained in terms of a central fluorine F', chemically equivalent protons and terminal fluorines, as illustrated by the structural formulas in Fig. 1. The high signal field shifts are consistent with an increasing  $\text{F} \dots \text{F}$  distance when another HF molecule is added. The gradual increase of the larger coupling constant  $^1J_{\text{HF}}$  indicates that at the same time the average proton position is shifted towards the terminal fluorines. By contrast, the smaller coupling constant  $^1J_{\text{HF}}'$  first decreases to 24 Hz in the case of  $[\text{F}(\text{HF})_2]^-$ , increases to 41 Hz in the case of  $[\text{F}(\text{HF})_3]^-$  and becomes small and no longer resolved in the case of  $[\text{F}(\text{HF})_4]^-$ .

The question then arises whether the coupling constants are positive or negative. Here, these signs can be determined from the differential widths of the individual line components of Fig. 1. The outer lines of the triplet of  $[\text{FHF}]^-$  are broader than the inner line, indicating that the transverse relaxation times  $T_2$  of the outer components are shorter than those of the inner line. It is well established that differential widths of multiplet line components arise from non-averaged interfering dipolar or chemical shield-

ing interactions when the rotational correlation times are increased by lowering the viscosity, for example by lowering the temperature [17]. To our knowledge, this effect has not yet been reported for  $[\text{FHF}]^-$ . Here, we assign this effect to an interference to the two dipolar  $\text{H}\dots\text{F}$  coupling tensors and an increase of the correlation time of rotational diffusion at 120 K. As contributions from the magnetic field inhomogeneity can be neglected the linewidths are proportional to the square of the effective dipolar interactions. Because of the linearity of the  $\text{F}\dots\text{H}\dots\text{F}$  hydrogen bonds the two dipolar coupling tensors are parallel and the effective dipolar  $\text{H}\dots\text{F}$  couplings cancel in the case of the center line of the triplet where the two fluorine's exhibit different spin states, i.e.  $\alpha(\text{F})\beta(\text{F}')$  or  $\beta(\text{F})\alpha(\text{F}')$ . Therefore, this line is sharp. By contrast, the two outer components are broad. As the gyromagnetic ratios of  $^1\text{H}$  and  $^{19}\text{F}$  are positive, the low-field component arises from  $\alpha(\text{F})\alpha(\text{F}')$  and the high field component from  $\beta(\text{F})\beta(\text{F}')$ , which is consistent with a positive sign of  $^1J_{\text{HF}}$ . By contrast, in the case of the signals of  $[\text{F}(\text{HF})_2]^-$  and  $[\text{F}(\text{HF})_3]^-$  the inner components are broader as compared to the outer components. Here, the two dipolar interactions  $\text{H}\dots\text{F}$  and  $\text{H}\dots\text{F}'$  do not completely cancel, but nevertheless the line widths of the components corresponding to  $\alpha(\text{F})\alpha(\text{F}')$  and  $\beta(\text{F})\beta(\text{F}')$  are larger than those corresponding to  $\alpha(\text{F})\beta(\text{F}')$  and  $\beta(\text{F})\alpha(\text{F}')$ . Since now the inner lines are broader than the outer lines, the smaller coupling constants  $^1J_{\text{HF}'}$  should be negative. Finally, we note an additional differential line width of the signal components which we attribute to an interference arising from the chemical shift anisotropy. A quantitative analysis of the linewidth effects is under progress.

### 3.1.2 $^{19}\text{F}$ NMR Spectra

The measurement of the  $^{19}\text{F}$  NMR spectra was difficult because of the presence of the solvent peaks. In order to obtain good signals for a given species its concentration was optimized. Therefore, the  $^{19}\text{F}$  NMR signals obtained at 120 K stem from different samples. It was checked, however, that the signal pattern and position was independent on the sample composition.

As expected [5],  $[\text{FHF}]^-$  contributes a doublet at  $\delta = 155.4$  ppm (Fig. 2a). Successive addition of HF leads to a small shift of the central fluorine signals to low field and to a strong shift of the terminal fluorine signal to high field (Fig. 2b and 2c). The relative intensity of the central to the terminal fluorine signals corresponds to the stoichiometry of the complexes. The terminal fluorine signals of  $[\text{F}(\text{HF})_2]^-$  and  $[\text{F}(\text{HF})_3]^-$  are split into doublets of doublets, and the central fluorine's into a triplet of triplets and a quartet of quartets, respectively. We assign an additional broad fluorine doublet at  $\delta = -191.4$  ppm to the terminal fluorine of  $[\text{F}(\text{HF})_4]^-$  (not shown); the corresponding signal of the central fluorine could not be identified; a candidate could be a small broad singlet at  $\delta = -148.2$  ppm.

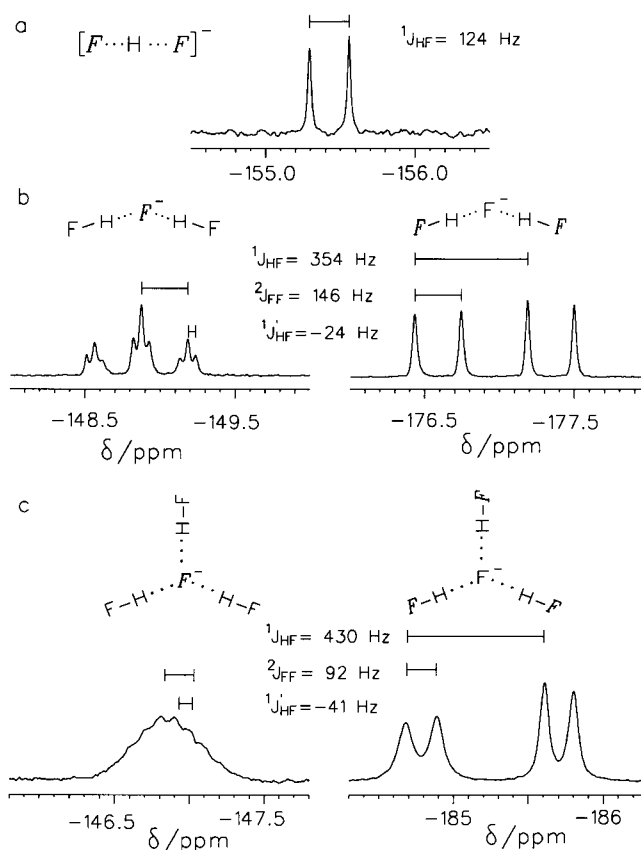


Fig. 2  
 $^{19}\text{F}$  NMR signals of HF-tetrabutylammonium fluoride complexes dissolved in  $\text{CDF}_3/\text{CDF}_2\text{Cl}$  at 130 K. Only the signals of the dominant species are shown. (a) Sample #3. (b) Sample #4. (c) Sample #1. in the freon mixture at 130 K

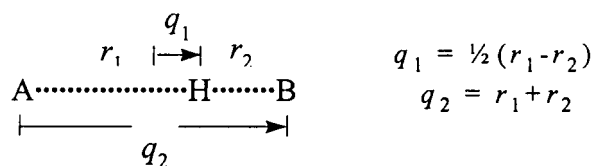
From the signals of the terminal fluorine's the coupling constants  $^1J_{\text{HF}}$  could be obtained and from the central fluorine signals the values of  $^1J_{\text{HF}'}$  which confirm the values from  $^1\text{H}$  NMR. However, in the case of  $[\text{F}(\text{HF})_2]^-$  and  $[\text{F}(\text{HF})_3]^-$ , unexpectedly both the central and terminal fluorine signals were additionally split into doublets by scalar two-bond couplings  $^2J_{\text{FF}} = 146$  Hz and 92 Hz, respectively.  $^2J_{\text{FF}}$  was not resolved in the case of the doublet at  $\delta = -191.4$  ppm tentatively assigned to  $[\text{F}(\text{HF})_4]^-$ . The assignment was justified by finding a coupling constant of  $^1J_{\text{HF}} = 480$  Hz which is substantially larger than in the case of  $[\text{F}(\text{HF})_3]^-$ . This value also helped to assign the corresponding proton signal in Fig. 1.

Finally, we calculated again the theoretical fluorine signal patterns and checked that the neglected of  $^2J_{\text{HH}}$ ,  $^3J_{\text{HF}}$ , and  $^4J_{\text{FF}}$  reproduces the experimental first-order line shapes of Fig. 2b and 2c. However, the calculations predict equal widths for all line components, whereas experimentally, again differential line widths are observed. In the case of the doublet of  $[\text{FHF}]^-$  the low-field line is slightly broader than the high field line (Fig. 2a). We assign this here to an interference of the dipolar  $\text{F}\dots\text{H}$  coupling with a collinear chemical shielding tensor. This effect is also seen in the signal of the terminal fluorine of  $[\text{F}(\text{HF})_3]^-$  (Fig. 2c) where the two high field components

are sharper. The additional effect of the dipolar coupling to the central fluorine leads to a broadening of the lines corresponding to the spin states  $\alpha(\text{H})\alpha(\text{F}')$  and  $\beta(\text{H})\beta(\text{F}')$  of the neighbouring nuclei, as compared to those of  $\alpha(\text{H})\beta(\text{F}')$  and  $\beta(\text{H})\alpha(\text{F}')$ . As the outer line components are broader than the adjacent inner line  ${}^2J_{\text{FF}}$  has to be positive. Again, a more quantitative analysis of these aspects is underway.

### 3.2 Results of Quantum Mechanical Calculations

The results of the various calculations of the optimized geometries, chemical shifts and coupling constants are included in Table 1. The data are visualized in Fig. 3 where we use as common abscissa the coordinate  $q_1 = 1/2(r_1 - r_2)$  corresponding to the deviation of the hydrogen bond proton from the hydrogen bond center as depicted in Scheme 1.



Scheme 1

For a given fluorine A,  $r_1$  corresponds to the distance to the proton, and  $r_2$  the distance of the proton to the distant fluorine B. As the proton is closer to the terminal fluorine  $q_1$  is, therefore, negative for these nuclei giving rise to the data on the left hand side of Fig. 3, whereas the data on the right hand side stem from the central fluorine's. We also include in Fig. 3 the experimental results discussed together in the following Section.

## 4. Discussion

Using low temperature liquid  ${}^1\text{H}$  and  ${}^{19}\text{F}$  NMR spectroscopy we have identified in addition to the well-known bifluoride ion  $[\text{FHF}]^-$  also the clusters  $[\text{F}(\text{HF})_2]^-$  and  $[\text{F}(\text{HF})_3]^-$ . In addition, we found some evidence for  $[\text{F}(\text{HF})_4]^-$ . For  $[\text{F}(\text{HF})_2]^-$  and  $[\text{F}(\text{HF})_3]^-$  chemical shifts and coupling constants are reported. Formally, these clusters exhibit a structure with a central fluoride ion hydrogen bonded to  $n$  equivalent HF units. It is remarkable that not only both one-bond coupling constants  ${}^1J_{\text{HF}}$  and  ${}^1J_{\text{HF}'}$  of the hydrogen bond proton with the terminal and central fluorine nuclei were observed but unexpectedly also a so far unknown two-bond coupling  ${}^2J_{\text{FF}}$  between the latter. As this coupling cannot be measured experimentally in the case of the bifluoride ion its existence has not yet been considered. The analysis of the NMR linewidth gives good arguments that  ${}^1J_{\text{HF}}$  and  ${}^2J_{\text{FF}}$  are positive and that  ${}^1J_{\text{HF}'}$  is negative. Thus, these quantities provide interesting information concerning the properties of the  $\text{F} \dots \text{H} \dots \text{F}$  hydrogen bonds in the different complexes. In order to understand these properties in more detail we

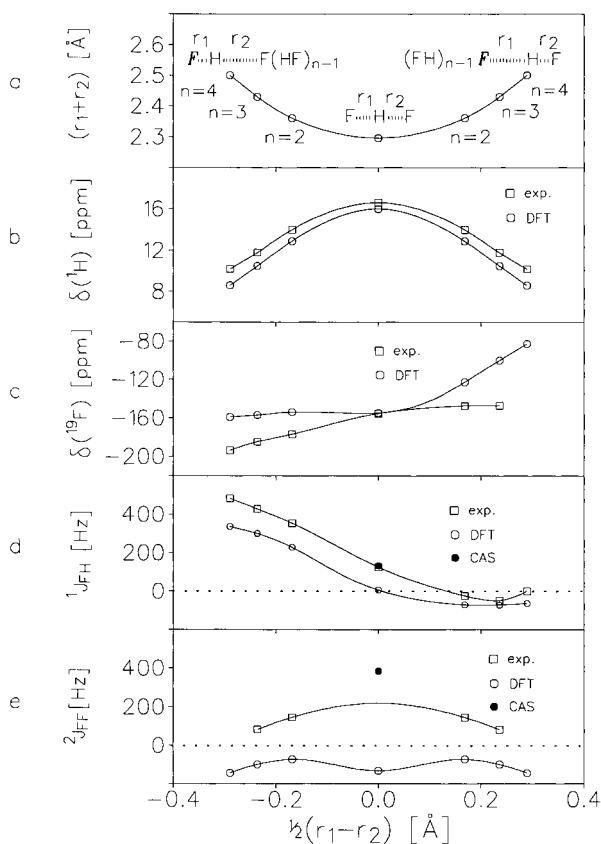


Fig. 3

Experimental and calculated properties of fluoride-HF as a function of the deviation  $q_1 = 1/2(r_1 - r_2)$  of the proton from the hydrogen bond center.  $q_1$  is positive for the central and negative for the terminal fluorine nuclei and obtained using ab initio calculations at the MP2/6-31+G(d,p) level (Table 1). (a) Calculated  $\text{F} \dots \text{F}$  distances  $q_2 = r_1 + r_2$ . (b)  ${}^1\text{H}$  and (c)  ${}^{19}\text{F}$  chemical shifts. (d) one bond and (e) two-bond coupling constants. For further description see text

have performed quantum mechanical ab initio calculations of the optimized cluster geometries at the MP2/6-31+G(d,p) level [7], of chemical shifts and coupling constants using Density Functional theory (DFT) [8] and MCLR-CAS methods [12–14]. At present, no attempt was made to correct for the anharmonic proton motion in the hydrogen bonds nor to include solvent or counterion effects.

### 4.1 Cluster Geometries and Chemical Shifts

The ab initio calculations at the MP2/6-31+G(p,d) led to the equilibrium geometries of the clusters presented in Table 1. The calculated symmetry of  $[\text{F}(\text{HF})_n]^-$ ,  $n = 1$  to 4 is  $D_{\infty h}$ ,  $C_{2v}$ ,  $D_{3h}$  and  $T_d$ , i.e. of the same type as the average solution symmetries obtained by NMR. The geometric data are in good agreement with the available MP2 values [2d] as well as those measured experimentally for the crystalline salts [1]. The finding that the structures of the anionic clusters are similar in the gasphase and in the solid state and not very sensitive to the type of the counterion makes it plausible that also the solution structures

are similar, which justifies to neglect the influence of the solvent in first order. Not justified is the complete neglect of the nuclear motion which is very anharmonic in the hydrogen bonds leading to strong deviations of the molecular geometry from the calculated equilibrium geometry. Therefore, we can only make qualitative and no quantitative comparisons of theoretical and experimental data.

In Fig. 3a we have plotted the F...F distance  $q_2 = r_1 + r_2$  as a function of the deviation of the proton from the hydrogen bond center  $q_1 = 1/2(r_1 - r_2)$  (see Scheme 2).  $q_1$  is negative for the terminal and positive for the central fluorine's. In the bifluoride ion  $q_1$  is zero, exhibiting a minimum F...F distance  $q_{2\text{min}}$ . The successive addition of HF molecules makes the hydrogen bond asymmetric, shifts the proton towards a terminal fluorine which is accompanied by an increase of the F...F distance. The correlation curve observed is similar to the one determined recently experimentally and theoretically for N...H...N hydrogen bond systems [18].

The associated evolution of the  $^1\text{H}$  chemical shifts is depicted in Fig. 3b. It is obvious that in the strong hydrogen bond regime these shifts are a measure of the F...F distance where the maximum low-field shift is obtained in the case of the shortest F...F distance. A detailed description of the relation between geometries and chemical shifts is given for the case of N...H...N hydrogen bonds in Ref. [18].

We note a good agreement of the calculated DFT  $^1\text{H}$  chemical shift values for the equilibrium geometries with the experimental values. This agreement is not satisfactory in the case of the calculations of the fluorine chemical shifts: only a very minor decrease of the latter was found experimentally in the series of  $n=2$  to 4, whereas the DFT calculations predict a similar but much more pronounced dependence. In this study it was not possible to elucidate the origin of this disagreement; we note, however, that preliminary calculations using the HF-IGLO method [11] gave similar results as the DFT method, indicating that either anharmonic effects or solvent effects may be responsible for the disagreement. For example, it is conceivable that  $\text{CDF}_3$  forms weak hydrogen bonds with the terminal fluorines, which depend on the cluster size.

The dependence of the one-bond H...F couplings as a function of the deviation  $q_1$  of the proton from the hydrogen bond center is interesting and plotted in Fig. 3d. If the proton is close to the fluorine considered,  $q_1$  is negative and the coupling constant positive. This is still true in the case of the symmetric bifluoride where  $q_1=0$ . By analysis of differential line widths of various multiplet lines experimental evidence was provided that for positive  $q_1$  the constant becomes negative. Then it goes through a minimum and vanishes eventually. Qualitatively, this "oscillation" is well reproduced by the values calculated using the DFT method although there is a large discrepancy between the absolute calculated and experimental values. A great part of this discrepancy must be attributed to the method of calculation employed. Despite very good

results for indirect spin-spin couplings between nuclei without lone pairs, accurate calculation of couplings with fluorine is still a challenge for DFT based methods [8e]. For example, the calculated one-bond couplings with fluorine are systematically shifted with respect to their experimental counterparts by about 110 Hz [8e]. However the experimental trends are usually well reproduced. Note that the value of this systematic deviation depends on the type of coupling studied.

The agreement between the experimental value for the bifluoride ion and the value calculated using the MCLR-CAS is, on the other hand, very satisfactory. If this agreement is real, it follows that the symmetry of  $[\text{FHF}]^-$  in solution is similar to that in the gasphase and that the proton motion is fairly harmonic. As the MCLR-CAS method is computationally much more demanding than the DFT method we could not explore in this study whether this method also predicts a minimum of the one-bond HF coupling in the negative region.

Let us now discuss the two-bond couplings  $^2J_{\text{FF}}$  between the terminal and the central fluorine's. To our knowledge, scalar couplings between two heavy atoms of a hydrogen bond have never been observed nor been calculated previously. We have experimental evidence that these couplings are positive. We note that the values are of the order of the geminal FCF couplings in saturated fluorocarbons [160–290 Hz], and even larger than the value of 95 Hz found for the fluorine-bridged anion,  $[\text{F}_3\text{B-F-BF}_3]^-$  [19]. Thus, the hydrogen bond clusters  $[\text{F}(\text{HF})_n]^-$  are better described in terms of a covalent charged molecule rather than as a fluoride ion solvated by HF groups. As discussed recently in detail [18] the bonding situation of Fig. 3a can be described in terms of a total hydrogen bond order of 1, but unequally distributed to the adjacent heavy atoms.

The results of the calculations confirm the existence of large values of  $^2J_{\text{FF}}$  as depicted in Fig. 3e. However, this type of coupling constitutes the most difficult problem for calculation by the DFT method. We note a large disagreement between the experimental values and the DFT values which are negative. The change of  $^2J_{\text{FF}}$  between  $[\text{F}(\text{HF})_2]^-$  and  $[\text{F}(\text{HF})_3]^-$  can be qualitatively reproduced, although the absolute values are negative, in contrast to the experimental values. However, for the symmetric complex  $[\text{FHF}]^-$  even the expected trend is not reproduced. The value for the bifluoride ion exhibits a minimum, whereas the MCLR-CAS value is positive and very large. Unfortunately, an experimental value can not be measured because of the equivalency of the fluorine nuclei, and furthergoing calculations were beyond the scope of this study.

## 5. Conclusions

Using low-temperature liquid state NMR spectroscopy we have identified various hydrogen bonded complexes between the fluoride ion and a varying number of HF molecules. These complexes do not exhibit only one-bond

H...F couplings which are positive at short and negative at larger H...F distances but also substantial positive two-bond F...F couplings. The latter have not yet been observed before and demonstrate the covalent character of the hydrogen bonds formed. The dependence of the coupling constants changes on the molecular structures is qualitatively reproduced in terms of preliminary ab initio DFT and CAS calculations. Therefore, the systems presented constitute useful models for testing methods of calculation of NMR-parameters of hydrogen bonded systems in solution. In the future, also solvent effects should be taken into account. Currently, we are studying effects of partial and full H/D substitution on the properties of the ions observed. For the understanding of these properties it will be necessary to take the anharmonic vibrational motion into account.

This work was supported by the Stiftung Volkswagenwerk, Hannover, the Russian Foundation of Basic Research (grant No. 96-03-32846), the Freie Universität Berlin, the Deutscher Akademischer Austauschdienst DAAD (Kennziffer A/97/53365), and the Fonds der Chemischen Industrie, Frankfurt. S. Kirpekar thanks the Danish natural science research council (grant No. 9600856). O. Malkina thanks the Slovak Grant Agency VEGA (grant No. 2/3008/97) for financial supports and all authors are indebted to Dr. V.G. Malkin for helpful discussions.

## References

- [1] (a) B.A.L. McGaw and J.A. Ibers, *J. Chem. Phys.* **39**, 2677 (1963). (b) W.W. Wilson, K.O. Christe, J. Feng, and R. Bau, *Can. J. Chem.* **67**, 1898 (1989). (c) W.W. Williams and L.F. Schneemeyer, *J. Am. Chem. Soc.* **95**, 5780 (1973). (d) O. Foss and K. Maartmann-Moe, *Acta Chem. Scand.* **A41**, 310 (1987). (e) F. Hibbert and J. Emsley, *Adv. Phys. Org. Chem.* **26**, 255 (1990) and references cited therein. (f) A.M. Panich, *Chem. Phys.* **196**, 511 (1995). (g) D. Mootz and D. Boenigk, *Z. Anorg. Allg. Chem.* **544**, 159 (1987). (h) A.R. Mahjoub, D. Leopold, and K. Seppelt, *Eur. J. Solid State Inorg. Chem.* **29**, 635 (1992). (i) J.D. Forrester, M.E. Senko, A. Zalkin, and D. Templeton, *Acta Crystallogr.* **16**, 58 (1963). (k) B.A. Coyle, L.W. Schroeder, and J.A. Ibers, *J. Solid. State Chem.* **1**, 386 (1970).
- [2] (a) V.C. Epa and W.R. Thorson, *J. Chem. Phys.* **93**, 3773 (1990). (b) J.H. Clark, J. Emsley, D.J. Jones, and R.E. Overill, *J. Chem. Soc. Dalton Trans.* 1219 (1981). (c) A. Karpfen and O. Yanovitskii, *J. Mol. Struct. (Theochem.)* **307**, 81 (1994); **314**, 211 (1994). (d) W.D. Chandler, K.E. Johnson, and J.L.E. Campbell, *Inorg. Chem.* **34**, 4943 (1995). (e) J. Almlöf, *Chem. Phys. Lett.* **17**, 49 (1972).
- [3] (a) K. Kawaguchi and E. Hirota, *J. Chem. Phys.* **87**, 6838 (1987). (b) K. Kawaguchi and E. Hirota, *J. Mol. Spectrosc.* **352/353**, 389 (1995). (c) I. Gennick, K.N. Harmon, and M.M. Potvin, *Inorg. Chem.* **16**, 2033 (1977).
- [4] C. Rieux, B. Langlois, and R. Gallo, *C.R. Acad. Sci. Ser.* **2**, 310, 25 (1990).
- [5] (a) F.Y. Fujiwara and J.S. Martin, *J. Amer. Chem. Soc.* **96**, 7625 (1974). (b) K.O. Christe and W.W. Wilson, *J. Fluorine Chem.* **46**, 339 (1990).
- [6] (a) N.S. Golubev and G.S. Denisov, *J. Mol. Struct.* **270**, 263 (1992). (b) N.S. Golubev, S.N. Smirnov, V.A. Gindin, G.S. Denisov, H. Benedict, and H.-H. Limbach, *J. Am. Chem. Soc.* **116**, 12055 (1994). (c) S.N. Smirnov, N.S. Golubev, G.S. Denisov, H. Benedict, P. Schah-Mohammadi, and H.-H. Limbach, *J. Am. Chem. Soc.* **118**, 4094 (1996). (d) N.S. Golubev, G.S. Denisov, S.N. Smirnov, D.N. Shchepkin, and H.-H. Limbach, *Z. Phys. Chem.* **196**, 73 (1996). (e) N.S. Golubev, S.N. Smirnov, P. Schah-Mohammadi, I.G. Shenderovich, G.S. Denisov, V.A. Gindin, and H.-H. Limbach, *Russian J. Gen. Chem.* **67**, 1150 (1997).
- [7] Gaussian 94, Revision D.3, M.J. Frisch, G.W. Trucks, H.B. Schlegel, P.M.W. Gill, B.G. Johnson, M.A. Robb, J.R. Cheeseman, T. Keith, G.A. Petersson, J.A. Montgomery, K. Raghavachari, M.A. Al-Laham, V.G. Zakrzewski, J.V. Ortiz, J.B. Foresman, J. Cioslowski, B.B. Stefanov, A. Nanayakkara, M. Challacombe, C.Y. Peng, P.Y. Ayala, W. Chen, M.W. Wong, J.L. Andres, E.S. Replogle, R. Gomperts, R.L. Martin, D.J. Fox, J.S. Binkley, D.J. Defrees, J. Baker, J.P. Stewart, M. Head-Gordon, C. Gonzalez, and J.A. Pople, Gaussian, Inc., Pittsburgh PA, 1995.
- [8] (a) deMon program: D.R. Salahub, R. Fournier, P. Mlynarski, I. Papai, A. St-Amant, and J. Ushio, in: "Density Functional Methods in Chemistry", ed. by J. Labanowski and J. Andzelm, Springer, New York, 1991; A. St-Amant and D.R. Salahub, *Chem. Phys. Lett.* **169**, 387 (1990). (b) V.G. Malkin, O.L. Malkina, M.E. Casida, and D.R. Salahub, *J. Am. Chem. Soc.* **116**, 5898 (1994). (c) V.G. Malkin, O.L. Malkina, L.A. Eriksson, and D.R. Salahub, in: "Modern Density Functional Theory: A Tool for Chemistry", Vol. 2, ed. by J.M. Seminario and P. Politzer, Elsevier, Amsterdam, 1995. (d) V.G. Malkin, O.L. Malkina, and D.R. Salahub, *Chem. Phys. Lett.* **221**, 91 (1994). (e) O.L. Malkina, D.R. Salahub, and V.G. Malkin, *J. Chem. Phys.* **105**, 8793 (1996).
- [9] J.P. Perdew and Y. Wang, *Phys. Rev. B* **33**, 8800 (1986).
- [10] J.P. Perdew, *Phys. Rev. A* **38**, 3098 (1988).
- [11] W. Kutzelnigg, U. Fleischer, and M. Schindler, in: "NMR-Basic Principles and Progress", Vol. 23, 165, Springer, Heidelberg, 1990.
- [12] (a) J. Olsen, D.L. Yeager, and P. Jørgensen, *J. Chem. Phys.* **91**, 381 (1989). (b) P. Jørgensen, H.J. Aa. Jensen, and J. Olsen, *J. Chem. Phys.* **89**, 3654 (1988).
- [13] B.O. Ross, *Adv. Chem. Phys.* **69**, 399 (1987).
- [14] T. Helgaker, H.J. Aa. Jensen, P. Jørgensen, J. Olsen, H. Ågren, T. Andersen, K.L. Bak, V. Bakken, O. Christiansen, T. Enevoldsen, B. Fernandez, P. Dahle, E.K. Dalskov, H. Heiberg, H. Hettema, D. Jonsson, S. Kirpekar, H. Koch, R. Kobayashi, A.S. de Meras, K.V. Mikkelsen, P. Normann, M.J. Packer, K. Ruud, T. Saue, P.R. Taylor, and O. Vahtras, DALTON, an electronic structure program, Release 1.0.1 (1997), <http://www.kjemi.uio.no/software/dalton>
- [15] (a) H.J. Aa. Jensen, P. Jørgensen, H. Ågren, and J. Olsen, *J. Chem. Phys.* **88**, 3834 (1988). (b) H.J. Aa. Jensen, P. Jørgensen, H. Ågren, and J. Olsen, *J. Chem. Phys.* **89**, 5354 (1988).
- [16] (a) J.W. Emsley, J. Feeney, and L.H. Sutcliffe, *High Resolution NMR Spectroscopy*, Vol. 1, Pergamon Press Oxford 1965. (b) R. Ditttrich, U. Weber, Th. Lenzen, and G. Haegle, University of Düsseldorf, 1997, code MINI-LA version 2.0, <ftp://ftp.uni-duesseldorf.de/pub/msdos/chemie/>.
- [17] (a) H. Shimidzu, *J. Chem. Phys.* **40**, 3357 (1964). (b) H. Rüterjans, E. Kaun, W.E. Hull, and H.-H. Limbach, *Nucleic Acids Res.* **10**, 7027 (1982). (c) R.H. Griffey, C.D. Poulter, Z. Amaizumi, S. Nishimura, and R.E. Hurd, *J. Am. Chem. Soc.* **104**, 5811 (1982). (d) M. Gueron, J.L. Leroy, and R.H. Griffey, *J. Am. Chem. Soc.* **105**, 7262 (1983).
- [18] (a) H. Benedict, H.H. Limbach, M. Wehlan, W.P. Fehlhammer, N.S. Golubev, and R. Janoschek, *J. Am. Chem. Soc.*, in press.
- [19] J.S. Hartman and P. Stilbs, *J. Chem. Soc. Chem. Comm.*, 566 (1975).

Presented at the Discussion Meeting of the Deutsche Bunsen-Gesellschaft für Physikalische Chemie "Hydrogen Transfer: Experiment and Theory" in Berlin, September 10th to 13th, 1997 E 9785